Published in: *Journal of Magnetism and Magnetic Materials* 421, pp. 194–206, 2017

Magnetic and magnetoresistance studies of nanometric electrodeposited Co films and Co/Cu layered structures: influence of magnetic layer thickness

S. Zsurzsa*, L. Péter, I. Bakonyi

Wigner Research Centre for Physics, Hungarian Academy of Sciences.
H-1121 Budapest, Konkoly-Thege út 29-33, Hungary

Abstract – The magnetic properties and the magnetoresistance behavior were investigated for electrodeposited nanoscale Co films, Co/Cu/Co sandwiches and Co/Cu multilayers with individual Co layer thicknesses ranging from 1 nm to 20 nm. The measured saturation magnetization values supported reasonably the validity of the nominal layer thicknesses. All three types of layered structure exhibited anisotropic magnetoresistance for thick magnetic layers whereas the Co/Cu/Co sandwiches and Co/Cu multilayers with thinner magnetic layers exhibited giant magnetoresistance (GMR), the GMR magnitude being the largest for the thinnest Co layers. The decreasing values of the relative remanence and the coercive field when reducing the Co layer thickness down to below about 3 nm indicated the presence of superparamagnetic (SPM) regions in the magnetic layers which could be more firmly evidenced for these samples by a decomposition of the magnetoresistance vs. field curves into a ferromagnetic and an SPM contribution. For thicker magnetic layers, the dependence of the coercivity (H_c) on magnetic layer thickness (d) could be described for each of the layered structure types by the usual equation $H_c = H_{co} + a/d^n$ with an exponent around $n = 1$. The common value of n suggests a similar mechanism for the magnetization reversal by domain wall motion in all three structure types and hints, at the same time, for the absence of coupling between magnetic layers in the Co/Cu/Co sandwiches and Co/Cu multilayers.

Keywords: magnetic properties; magnetoresistance; electrodeposition; nanoscale magnetic layers;

PACS numbers: 75.70.Cn, 75.47.De, 81.15.Pq

*****Corresponding author (Ph.D. student at Eötvös University, Budapest). E-mail: zsurzsa.sandor@wigner.mta.hu

1. Introduction

The application of the giant magnetoresistance (GMR) effect [1,2] in magnetic field sensors has been greatly advanced by the introduction of the exchange-coupled GMR spin-valve concept [3]. The basic structure of a spin-valve is a sequence of a ferromagnetic (FM) layer 1, a non-magnetic (NM) spacer layer, an FM layer 2 and an antiferromagnetic (AF) layer (schematically, FM1/NM/FM2/AF), each sublayer being in intimate contact with the neighbouring layer(s) [4]. A typical sequence is for example Ni-Fe/Cu/Co/Ni-Mn. The two FM layers are uncoupled or only weakly coupled through the spacer layer. Therefore, whereas FM layer 2 is strongly pinned by the AF layer and keeps its magnetization orientation fixed as determined by the FM2/AF interface, the orientation of the magnetization of the magnetically soft FM1 layer (also called "free" layer) can be easily changed by a relatively small external magnetic field. In this manner, the magnetizations of the FM1 and FM2 layers can be aligned at practically any inclination angle. Specifically, a parallel alignment corresponds to a low-resistance state whereas in the antiparallel aligned state, due to the GMR effect in the FM1/NM/FM2 structure, the resistance is significantly higher. The resistance difference of the two alignment states can be used for the detection of a magnetic field (e.g., the stray field between differently oriented magnetic regions) and this is the basis for using the GMR spin-valve structure, e.g., in read-out heads of hard-disk drives [5].

The GMR effect originally discovered in FM/NM multilayer structures [1,2] is the highest when the adjacent layer magnetizations are antiparallel aligned [6-8]. In physically deposited multilayer structures, this can be achieved by choosing spacer layer thicknesses ensuring an AF coupling between adjacent layers which occurs at the so-called AF maxima [9-11]. Specifically, for Co/Cu multilayers, at the first AF maximum (at about 1 nm spacer thickness), the AF coupling is very high and strong magnetic fields (as high as 5 to 10 kOe) [9,11] can only reverse the magnetizations to achieve the parallel alignment (low-resistance state). At the second AF maximum for the same multilayers (typically at 2 nm spacer layer thickness), the GMR is reduced by a factor of two, but since the saturation field is reduced by a factor of 10, there is a significant gain in field sensitivity [9,11]. However, the saturation field is still typically 0.5 kOe here whereas even lower saturation fields are required for sensor applications [5].

A possible solution to comply with this requirement was the elaboration of the spin-valve structure [3] which has, indeed, found successfully application in sensors. Another concept was also proposed to reach high GMR at sufficiently low magnetic fields by the so-called

pseudo spin-valve [12,13]. Such a structure can be formed by the repetition of a [FM_S/NM/FM_h/NM] quadrilayer [12] to build up a multilayer or can simply consist of a FM_S/NM/FM_h trilayer sandwich [13]. In both pseudo spin-valve versions, the coercivity of the FM_S layer (soft layer) is smaller than the coercivity of the FM_h layer (hard layer) whereas the NM layer thickness is chosen to exhibit a coupling between the FM1 and FM2 layers as small as possible. After saturating both FM layers in one direction and changing the magnetic field direction to the opposite, first the FM_S layer magnetization will reverse whereas the FM_h layer magnetization remains in the original orientation until its coercive field is reached. Thus, in the magnetic field range between the FM_S and FM_h coercivities, the magnetizations of the two kinds of magnetic layers are antiparallel aligned and a significant GMR effect can occur when passing a current through this pseudo spin-valve structure. The different coercivities can be achieved either by appropriately choosing the individual magnetic layer thicknesses or their composition (e.g., Co and Ni-Fe).

In Section 6.3 of Ref. 4, we have summarized the attempts to produce a spin-valve sandwich structures by electrodeposition [14-19]. According to the basic idea of Attenborough et al. [14-16], in the core of the sandwich, an artificial antiferromagnet (AAF) was designed by preparing a Co(2.7nm)/Cu(3.2nm)/Co(2.7nm)/Cu(3.2)/Co(2.7nm) layered structure with thin Co layers and thin Cu layers, the latter intended to ensure a strong AF coupling between the Co layers. On both sides of this core structure, a thick Co layer (10 nm) was grown which was separated by a thick Cu layer (4.7 nm) from the core, the latter employed with the purpose of magnetically decoupling the outer thick Co layers from the core structure. The whole structure indeed exhibited a pseudo spin-valve behavior in that a clear plateau could be observed in the *MR(H)* curve (with a maximum GMR of about 5 %) and clear steps in the *M(H)* curve [14-16]. However, a critical evaluation [4] of these results led to the conclusion that actually an AAF structure was not formed in the core. This conclusion is mainly supported by the summary of experimental results on electrodeposited Co/Cu multilayers [20,21] which reveals that the GMR magnitude does not exhibit an oscillatory behavior, but rather a monotonous increase with increasing Cu spacer thickness. Therefore, the thin spacer layer thickness (2.3 nm) used by Attenborough et al. [14-16] is not expected to mediate an AF coupling. Shima et al. [17] prepared the same layered structure with almost equivalent layer thicknesses and on an identical substrate. Although distinct MR switching curves were observed for both positive and negative magnetic fields, the maximum magnetoresistance was only slightly above 1 %. Therefore, Shima et al. [17] concluded that

their observed magnetoresistance may have stemmed from domain wall magnetoresistance. Pasa and coworkers [18,19] have also attempted the preparation of similar electrodeposited sandwich structures as pseudo spin-valves, but their results neither showed convincingly a plateau behavior of the *MR(H)* curves.

As noted above, the basic problem is that since there is no evidence for an AF coupling in electrodeposited Co/Cu multilayers, but rather for the absence of such a coupling [20,21], an AAF structure cannot be prepared by this technique. Therefore, for achieving a pseudo spin-valve behavior in electrodeposited layered structures, the realization of uncoupled magnetic layers with different coercivities should be pursued instead.

From an analysis of the evolution of both the GMR magnitude and the coercivity with spacer layer thickness [21], it could be concluded that in electrodeposited Co/Cu multilayers, fully uncoupled magnetic layers can be achieved above a certain Cu layer thickness only since for small spacer thicknesses an FM coupling cannot be excluded. Having uncoupled magnetic layers in a layered magnetic nanostructure, the coercivity of the magnetic layers can be controlled by their thickness since the most typical behavior in magnetic thin films is a monotonous decrease of the coercivity with increasing thickness [22,23].

Therefore, it was the purpose of the present work to study the variation of the coercivity of Co layers with thickness. For this purpose, we have prepared various electrodeposited nanometric layered structures from Co thin films via Co/Cu/Co sandwiches to Co/Cu multilayers. For the latter two structures, the Cu spacer layer thickness was chosen 5 nm which was expected to be sufficient to ensure a decoupling of the adjacent magnetic layers [21]. For comparing the behavior of the three kinds of magnetic nanostructure, magnetic and magnetoresistance measurements were carried out at room temperature for Co layer thicknesses ranging from 1 nm to 20 nm.

2. Experimental

The nanometric electrodeposited Co thin films, Co/Cu/Co sandwiches as well as the Co/Cu multilayers were electrodeposited from a aqueous electrolyte containing 0.74 mol/l $CoSO_4$, 0.010 mol/l $CuSO_4$, 0.3 mol/l Na_2SO_4, 0.25 mol/l H_3BO_3, and 0.15 mol/l H_3NO_3S. The bath composition was very similar to the one used in our previous work on studying the initial growth stages of electrodeposited Co/Cu multilayers [24].

All the samples were deposited on a [100]-oriented, 0.26 mm thick Si wafer covered with a 5 nm Cr and a 20 nm Cu layer by evaporation. The purpose of the chromium layer was to

ensure adhesion and the Cu layer was used to provide an appropriate electrical conductivity for the cathode surface. Electrodeposition was carried out in a tubular cell of 8 mm × 20 mm cross section at room temperature with an upward facing substrate placed at the bottom of the cell [4,25]. This arrangement ensures a lateral homogeneity of the deposits and helps to avoid edge effects.

Based on our experience in studying the initial growth stages of electrodeposited Co/Cu multilayers [24], the electrodeposition process was always started with the deposition of a 2.5 nm thick Cu layer on the Si/Cr/Cu substrate. One aim of depositing such an initial Cu layer is to get rid of, at least partially, the influence of the native oxide of the evaporated Cu layer before the deposition of the first Co layer. Since the deposition of the magnetic layered structures of interest was always started with a Co layer, the observed detrimental influence of the native oxide layer on the Co nucleation [24] could be significantly reduced in this manner. The other beneficial effect is the reduction of the Cu content in the first Co layer due to a depletion of the electrolyte at the cathode surface before the Co deposition, hence reducing any possible difference between the first and upcoming Co layers. After completing the deposition of the magnetic layered structure in the form a single Co thin film or a Co/Cu/Co sandwich, a protective Cu layer of 5 nm thickness was immediately electrodeposited on top of it from the same bath. The same 5 nm thick Cu layer was used as spacer between the magnetic layers in both the Co/Cu/Co sandwiches and the Co/Cu multilayers (for the latter, the last 5 nm thick Cu layer served simultaneously as a protective surface layer). The 5 nm thickness of the Cu spacer layer was chosen on the basis of our previous work [21] according to which at this spacer thickness we can already expect a more or less perfect decoupling of the adjacent magnetic layers. In the nanometric structures, the magnetic layer thickness d_{Co} was varied from 1 nm to 20 nm. For the Co/Cu multilayers, the bilayer repeat number was chosen to give a total multilayer thickness d_{ML} of about 100 nm.

Accordingly, the electrodeposited magnetic nanostructures investigated here were as follows: (i) single Co thin films as Si/Cr/Cu//Cu(2.5nm)/[Co(d_{Co})]/Cu(5nm); (ii) Co/Cu/Co sandwiches as Si/Cr/Cu//Cu(2.5nm)/[Co(d_{Co})/Cu(5nm)/Co(d_{Co})]/Cu(5nm) and (iii) Co/Cu multilayers as Si/Cr/Cu//Cu(2.5nm)/[Co(d_{Co})/Cu(5nm)]×N. The double slash symbol (//) refers to the transition between physically deposited and electrodeposited layers. The actual nanometric magnetic layered structure of interest is included between the square brackets []. For simplicity, the above three kinds of investigated nanometric magnetic layered structure will be denoted in the following as (i) Co(d_{Co}) thin film, (ii) Co(d_{Co})/Cu(5nm)/Co(d_{Co})

sandwich and (iii) [Co(d_{Co})/Cu(5nm)]×N multilayer, respectively.

For the present study, the electrodeposited nanometric layered structures were prepared using galvanostatic/potentiostatic (G/P) deposition [4,25] in which the magnetic layer is deposited by controlling the deposition current (G mode), whereas the non-magnetic layer (pure Cu) is deposited by controlling the deposition potential (P mode). The deposition of the magnetic layer was carried out at a current density of -56 mA/cm^2. For the Cu layer deposition, the deposition potential was kept at -613 mV with respect to a saturated calomel electrode (SCE). This electrochemically optimized potential for Cu [4] was used to ensure that neither the dissolution of the Co layer, nor Co incorporation into the Cu layer can occur. At the same time, this condition also ensures that the nominal layer thicknesses calculated by Faraday's law for both the magnetic and non-magnetic layers agree fairly well with the actual values. In the calculations of the nominal layer thicknesses, a current efficiency of 100% was assumed. This is generally accepted for Cu deposition carried out at the limiting current and for the Co deposition, it was estimated to be about 96 % in our previous work [26]. Detailed structural studies on electrodeposited Co/Cu multilayers [27,28] have indeed demonstrated a fairly good agreement (within about 10 %) of the nominal and actual layer thicknesses.

The room-temperature magnetoresistance (MR) was measured as a function of the external magnetic field (H) up to H = 1.7 kOe. The MR ratio was defined with the formula $MR(H) = (R_H - R_0)/R_0$, where R_0 is the resistance of the sample in zero external magnetic field and R_H is the resistance in an external magnetic field H. The magnetoresistance was determined in the field-in-plane/current-in-plane (FIP/CIP) geometry in both the longitudinal (LMR, magnetic field being parallel to the current) and the transverse (TMR, magnetic field being perpendicular to the current) configurations with a four-point-in-line probe placed symmetrically on the 8 mm × 20 mm sample.

Furthermore, magnetic measurements were also performed for the nanometric magnetic layered structures while being on their substrates at room temperature with a vibrating sample magnetometer (VSM). Before measuring the *M(H)* curves in a selected field range, a magnetic field of H = 6.5 kOe was used first to saturate the samples in their plane. The correction due to the Si/Cr/Cu substrate and the sample holder was carried out by measuring a Si/Cr/Cu substrate without any electrodeposited magnetic layer on it.

In order to increase the signal strength due to the very thin magnetic layers, the whole sample together with its substrate with a lateral size of 8 mm × 20 mm was inserted into the VSM. The large rectangular sample was attached to the sample holder symmetrically and with

its long axis being horizontal. The sample holder was placed at the same vertical position in the VSM as for the measurement of the usual sample sizes (5 mm × 5 mm). Since in such a case most of the sample is out of the homogeneity range of the detection coil, the following test was carried out. For a [Co(20nm)/Cu(5nm)]×4 multilayer, the M(H) curve was measured for the whole 8 mm × 20 mm sample as described above and then a central part of 5 mm × 5 mm was cut out of the sample and that piece was also measured. The latter sample size being within the homogeneity range provides the true *M(H)* curve of the sample. The agreement between the two *M(H)* curves, including the coercivity values and the scaled magnetic moments, was very satisfactory as demonstrated in Fig. 1. This test result justifies our procedure that the whole electrodeposited sample of 8 mm × 20 mm size was measured in the VSM.

3. Magnetic and magnetoresistance results

3.1 Co thin films

The magnetization curves are shown in Fig. 2 for Co(1nm) and Co(5nm) thin films. Whereas the shape of the hysteresis loop indicates FM behavior for d_{Co} = 5nm, a small superparamagnetic (SPM) contribution may also be present for d_{Co} = 1 nm, as indicated by the smaller remanence (this will be discussed further later). The Co thin films with layer thicknesses between 1 and 5 nm exhibited a similar hysteresis loop as that for d_{Co} = 1 nm whereby the sign for an SPM contribution progressively reduced with increasing d_{Co} and above 5 nm a clear FM behavior was only observed.

The evolution of the magnetoresistance characteristics with Co layer thickness is represented by the MR(H) curves shown in Fig. 3. The measured *MR(H)* curves for d_{Co} = 5 nm (Fig. 3a) and for larger Co layer thicknesses (Fig. 3b) correspond to that expected for homogeneous FM metals and alloys which exhibit the so-called anisotropic magnetoresistance (AMR) [29,30] behavior. This corresponds well to the magnetic behavior of Co thin films for layer thicknesses at and above 5 nm (Fig. 2). We can observe that both the LMR and TMR components exhibit a rapid variation in small magnetic fields until magnetic saturation is achieved at about H_S = 0.25 kOe after which the *MR(H)* curve remains approximately constant (due to the so-called paraprocess [31], a slight, nearly linear decrease of MR beyond H_S may often be observed).

The magnitude of the AMR is defined as the difference between the saturation values of the LMR and TMR components (AMR = LMR_S –TMR_S) [26,29,30]. Since the MR behavior of most FM metals and alloys is characterized by $LMR_S > 0$ and $TMR_S < 0$, we usually have AMR > 0. It appears from the MR results that for these Co thin films the magnitude of both the LMR_S and TMR_S components (and, thus, of the AMR) increases with d_{Co}. This is due to the progressively reducing shunting effect of the evaporated and electrodeposited non-magnetic layers into which the magnetic Co layer is embedded since the AMR effect derives only from the spin-dependent electron scattering effects within the FM Co layer.

For a magnetically isotropic material, the ratio TMR_S/LMR_S is expected to be -1/2 [26]. Apparently, this ratio is different from -1/2 for the Co thin films with layer thicknesses of 5 nm and larger (Fig. 3) and this indicates some magnetic anisotropy in the film plane. Such a magnetic anisotropy may occur due to the laterally dilated state of the magnetostrictive Co film when sandwiched between Cu layers and also due to the inherent stresses in deposited thin layers.

The *MR(H)* curves of the Co(1nm) thin film exhibit somewhat different behavior (Fig. 3). Evidently, saturation is not achieved even beyond magnetic fields where the thicker Co films are already saturated. The non-saturating character of the *MR(H)* curves may arise [4,32] from the presence of SPM regions in the Co(1nm) thin film, in agreement with the suggestion provided by the *M(H)* loop of the same Co thin film (Fig. 2). The other distinct feature is that whereas the magnitude of the TMR_S component in the highest magnetic fields applied is nearly as high as the TMR_S value for the Co(5nm) thin film, the LMR(H) component for the Co(1nm) thin film is much smaller and, after a small initial rise at low magnetic fields, it becomes later even negative. This hints at the presence of a small GMR contribution which may arise from spin-dependent electron scattering events for electron paths between FM and SPM regions [4,32]. We have already discussed in a previous study [24] that in very thin Co layers, when inserted between Cu layers, a GMR effect may occur if the Co layer is broken up into non-percolating regions since then there may be conducting paths between such regions via the surrounding Cu layers. In the present study, the Co layer thickness is even smaller than in the previous work [24] so that blocking of Co nucleation at some substrate surface sites may effectively contribute to the formation of a non-percolating Co layer at such a small effective Co layer thickness. The shape of the *MR(H)* curve and, to a lesser extent, also of the *M(H)* curve for the Co(1nm) thin film indicate that both FM and SPM regions occur in this magnetic layer.

The *MR(H)* curves for Co layer thicknesses between d_{Co} =1 nm and 5 nm showed a gradual transition from the Co(1nm) film to Co(5nm) film (Fig. 3a): with increasing d_{Co}, the *MR(H)* curves became saturated in progressively lower magnetic fields and the saturation value of LMR also increased continuously towards positive values.

3.2 Co/Cu/Co sandwiches

The magnetization curves are shown in Fig. 4 for Co/Cu/Co sandwiches with Co layer thicknesses d_{Co} = 1 and 5 nm. The general behavior of the hysteresis loops is the same as described above for the Co thin films with identical d_{Co} values (Fig. 2), i.e., clear FM characteristics for d_{Co} = 5 nm whereas the hysteresis loop for d_{Co} = 1 nm seems to show some SPM contribution as well. The *M(H)* curves of Co/Cu/Co sandwiches with layer thicknesses between 1 and 5 nm exhibited hysteresis loops in between those shown in Fig. 4 whereas for d_{Co} values higher than 5 nm, a clear FM behavior with square-shaped hysteresis was found.

The results of magnetoresistance measurements for the Co/Cu/Co sandwich with d_{Co} = 1 nm is shown in Fig. 5. Since both LMR and TMR are negative in the whole magnetic field range, this is a clear indication of a dominant GMR contribution to the observed MR (the difference between the LMR_S and TMR_S values indicates an AMR contribution as well which is, however, small due to the low Co layer thickness). Furthermore, it can be observed that MR saturation is not achieved even at the highest magnetic field applied in the case of the Co(1nm)/Cu(5nm)/Co(1nm) sandwich, again in agreement with the corresponding result for the Co(1nm) thin film (Fig. 3a). This is an indication of a SPM contribution to the observed GMR in addition to the FM contribution (the latter termed as the classical FM/NM multilayer GMR term). Although the GMR_{SPM} term is much smaller than the GMR_{FM} term, it unambiguously indicates the presence of SPM regions in the Co(1nm)/Cu(5nm)/Co(1nm) sandwich. This corresponds again well to the somewhat sheared hysteresis loop of this sandwich (cf. Fig. 4).

For the Co/Cu/Co sandwiches with d_{Co} = 5 and 10 nm, the *MR(H)* curves (Fig. 6a) also clearly indicate the presence of a GMR contribution (both LMR_S and TMR_S are negative) which arises from spin-dependent scattering events due the FM/NM/FM layered structure since saturation is achieved in fairly low magnetic fields. Evidently, due to the constancy of

the *MR(H)* curves of the sandwiches Co(5nm)/Cu(5nm)/Co(5nm) and Co(10nm)/Cu(5nm)/Co(10nm) above a small saturation field, the observed *MR(H)* data correspond completely to the GMR_{FM} term in these samples.

In addition, there is also an AMR contribution in both samples as revealed by the difference of their LMR_S and TMR_S values (Fig. 6a) which arises from spin-dependent scattering within the FM layers. It can also be observed in Fig. 6a that with increasing d_{Co} in the Co/Cu/Co sandwiches, the AMR term becomes also larger. However, the *MR(H)* behavior of the Co(20nm)/Cu(5nm)/Co(20nm) sandwich (Fig. 6b) indicates a different case with respect to the other two sandwiches shown in Fig. 6a since the signs of the LMR_S and TMR_S components are different for d_{Co} = 20 nm. This means that for this sandwich, the AMR term becomes comparable to the GMR_{FM} contribution. However, the shape of the LMR(H) curve at low fields (a slight maximum) and the fact that the magnitude of the LMR_S is well below that of the TMR_S component hints at the presence of a GMR_{FM} contribution as well. The larger and larger AMR term in comparison with GMR as d_{Co} increases in the Co/Cu/Co sandwiches is due to the fact that larger and larger fractions of the sandwich consist of the FM metal whereas the number of FM/NM interfaces which is the source of the GMR term does not change (or we may also say that the number of FM/NM interfaces per unit thickness is reduced with increasing d_{Co}).

As noted above, the magnitude of the AMR contribution is defined as the difference between the saturation values of the LMR and TMR contributions ($AMR = LMR_S - TMR_S$). From the measured LMR(H) and TMR(H) data, we can also eliminate the AMR contribution and this way we can determine the isotropic GMR via the expression $GMR_{is} = (1/3)\ LMR + (2/3)\ TMR$ [4,26]. The $GMR_{is}(H)$ curve is shown in Fig. 6b by the red line for the Co(20nm)/Cu(5nm)/Co(20nm) sandwich. In the following discussions, the quantity GMR_{is} will denote only the saturation value of the isotropic GMR defined by $GMR_{is} = (1/3)\ LMR_S + (2/3)\ TMR_S$. Since there is no SPM contribution, the GMR_{is} term will refer to the GMR_{FM} contribution only.

The *MR(H)* curves for sandwiches with Co layer thicknesses between 1 nm and 5 nm exhibited a continuous transition in that the non-saturating SPM contribution progressively died out with increasing d_{Co}.

3.3 Co/Cu multilayers

Figure 7 shows the magnetization curves for the Co/Cu multilayers with Co layer thicknesses d_{Co} = 1 and 5 nm and with a total multilayer thickness of about 100 nm. The hysteresis loops are very similar to those of the corresponding Co/Cu/Co sandwiches: for d_{Co} = 1 nm, the hysteresis loop is somewhat sheared possibly due to a small SPM contribution whereas square-shaped loops typical for a fully FM phase are present for at least 5 nm thick Co layers. The *M(H)* loops for Co layer thicknesses between 1 nm and 5 nm showed a gradual transition between the two curves shown in Fig. 7.

The magnetoresistance curves of these multilayers (Figs. 8 and 9) are again in full conformity with their *M(H)* loops. The multilayers with large Co layer thicknesses (d_{Co} = 5 nm and 20 nm, cf. Fig. 9) exhibit clearly an FM contribution only to the GMR but there is evidently an increasing AMR contribution as well for larger Co layer thicknesses, similarly to the Co/Cu/Co sandwiches. For d_{Co} = 1 nm, the non-saturating character of the *MR(H)* curves (Fig. 8a) indicates the presence of a GMR_{SPM} contribution. The *MR(H)* data for Co/Cu multilayers with Co layer thicknesses between 1 nm and 5 nm showed a gradual transition between the data for d_{Co} = 1 and 5 nm, i.e., the SPM contribution continuously disappeared for larger Co layer thicknesses.

For magnetic nanostructures with non-saturating *MR(H)* curves, the FM and SPM contributions can be decomposed according to a standard procedure [4,32] by fitting the measured *MR(H)* data to a Langevin function in the high-field region (i.e., for magnetic fields where the *MR(H)* hysteresis loop already closes). The high-field region corresponds to the GMR_{SPM} contribution and subtracting this contribution from the experimental data, we get the GMR_{FM} contribution in the low-field region. The larger magnitude of the magnetoresistance of the Co(1nm)/Cu(5nm) multilayer with respect to the Co(1nm) thin film and the Co(1nm)/Cu(5nm)/Co(1nm) sandwich provides *MR(H)* data with an accuracy that enables already a good fit to the Langevin function, especially when carrying out the *MR(H)* measurements up to H = 8 kOe. The results of the decomposition procedure into FM and SPM contributions to the GMR are shown for the Co(1nm)/Cu(5nm) multilayer in Fig. 8b. Although the GMR_{SPM} term is much smaller than the GMR_{FM} term, it unambiguously indicates the presence of SPM regions in the Co(1nm)/Cu(5nm) multilayer. This corresponds well to the somewhat sheared hysteresis loop of this multilayer (cf. Fig. 7).

The successful interpretation of the non-saturating *MR(H)* data for the Co(1nm)/Cu(5nm) multilayer justifies our above discussion about the presence of SPM regions in the magnetic layers of Co(1nm) thin films and Co(1nm)/Cu(5nm)/Co(1nm) sandwiches as well.

The typical SPM moments obtained previously on electrodeposited Co/Cu multilayers [32-36] ranged from 1000 to 10000 μ_B. In conformity with these former results, from the decomposition analysis of the *MR(H)* data for the present Co(1nm)/Cu(5nm) multilayer, the average magnetic moment of an SPM region was found to be 3600 μ_B. This value corresponds approximately to an SPM region of the size 1 nm × 4 nm × 4 nm (here, we have assumed that one Co atom has a magnetic moment of 1.7 μ_B, 1 nm corresponds to about 5 atomic layers and the SPM region has the typical thickness of the magnetic layer, i.e., 1 nm).

It appeared in the above discussions that the shape of the *MR(H)* curves (i.e., their non-saturating character) provided more direct hints at the presence of SPM regions in the thin Co layers than the *M(H)* curves of the same magnetic nanostructures. The larger sensitivity of the *MR(H)* data to the SPM regions with respect to the sensitivity of the *M(H)* data has already been discussed in our previous works [32,33] on a comparative study of the magnetic and magnetoresistance properties of electrodeposited Co/Cu multilayers. Namely, the *M(H)* data are sensitive only to the ratio of the volume fractions of the FM and SPM regions in the sample. However, the *MR(H)* data are rather sensitive to the relative arrangement of the SPM and FM regions with respect to each other since this strongly influences the relative weight of spin-dependent scattering events coming from electron paths between SPM and FM regions (GMR_{SPM} term) and between FM and FM regions (GMR_{FM} term).

Previous reports by other researchers on both electrodeposited [36,37] and sputtered [38-40] Co/Cu multilayers with very thin Co layers around 1 nm and below gave further support to our findings and conclusions concerning the appearance of SPM regions in such multilayers. Namely, it turned out from these studies when increasing the Co layer thickness in the subnanometer range that whereas the *M(H)* curves evolve from a hysteresis-less behavior to the appearance of a clear hysteresis, i.e., the formation of FM regions, the *MR(H)* curves remain still strongly non-saturating with negligible hysteresis. Along this line, Spizzo et al. [38] concluded that since the *M(H)* and *MR(H)* curves evolve differently with Co layer thickness, they should have different origin and have given a very reasonable explanation for this behavior. Namely, in order to understand this difference, one has to consider that the electronic mean free path related to spin flipping is of the order of a few tens of nanometers. Therefore, spin-dependent scattering processes have to take place on a comparable length

scale in order to produce a GMR effect. Consequently, GMR is influenced above all by the magnetic reorientation over a nanometric scale. On the other side, magnetization measurements are sensitive to the average magnetic moment of the sample and are mainly affected by the ferromagnetic response over large scale. This underpins the importance of the possibility of a GMR measurement on the multilayer in revealing more sensitively the presence of SPM regions than the bulk magnetic measurements. It also explains why it is much harder to identify the presence of a small SPM fraction in a partially discontinuous Co thin film where the GMR effect is missing (or can manifest itself only rather faintly in the *MR(H)* measurement if the Co layer is inserted between two Cu layers).

4. Evolution of magnetic and magnetoresistance behavior with Co layer thickness

4.1 Magnetization

From the lateral size of the electrodeposited layered structures and the measured saturation magnetic moments, we could determine the magnetization per unit area for each sample. This quantity can be written as $D_{Co} \cdot M_S$ where D_{Co} is the total Co layer thickness in the layered structure and M_S is the saturation magnetization of Co. Accordingly, the magnetization per surface area should be proportional to D_{Co} in any of the three kinds of magnetic nanostructure (Co thin films, Co/Cu/Co sandwiches and Co/Cu multilayers). Therefore, the $D_{Co} \cdot M_S$ data are plotted in Fig. 10a as a function of the total magnetic layer thickness for all three layered nanostructures.

Although the stable crystalline phase of Co is the hexagonal close-packed (hcp) structure and no direct structural studies have been performed on the present electrodeposited samples, they probably exhibit, at least up to a certain thickness of the individual Co layers, a face-centered cubic (fcc) structure [41], especially when stabilized by adjacent Cu layers from both sides [27,28,42]. Even if a small hcp-fraction in the Co layers cannot be excluded for larger thicknesses, according to the careful measurements of Liu et al. [41] on epitaxially-grown fcc and hcp Co thin films, the magnetic moments are identical within an experimental error of ±3.5 % for the two phases. This has been confirmed also by the recent work of Topolovec et al. [43] on electrodeposited Co films. All this is also in agreement with earlier results according to which the magnetic moment difference between the bulk hcp and fcc phases of Co is about 1.8 % only [44].

The thin dashed reference line in Fig. 10a represents the evolution of $D_{Co} \cdot M_S$ with Co layer thickness by using the measured room-temperature Co saturation magnetization of 159 emu/g [41]. We can see that the data in Fig. 10a are scattered, more or less randomly, around the reference line which is an indication that, on the average, our nominal Co layer thicknesses correspond well to the actual values.

According to Fig. 10a, the Co/Cu multilayer data follow fairly well the expected trend. Since the data for the Co thin films and the Co/Cu/Co sandwiches are gathered mostly for lower total Co layer thicknesses, these two datasets are shown separately on an enlarged scale in Fig. 10b. We can see that whereas the Co/Cu/Co sandwich data still fairly well scatter around the reference line, there is a systematic downward deviation of the experimental data for the Co thin films. This may partly come from the very small VSM signal due to the small amount of magnetic material in these Co thin films, all this resulting in a larger experimental uncertainty for this group of samples. In addition, the clearly systematic downward deviation of $D_{Co} \cdot M_S$ can also indicate that the nucleation of the very first Co layer may indeed be hindered which then results in the appearance of SPM regions; since their magnetization contribution is not included in the measured $D_{Co} \cdot M_S$ values due to the low magnetic fields applied, this may also be a reason for the downward deviation.

It should be noted that in a recent careful experimental work on Co thin films electrodeposited inside a SQUID magnetometer [43], a significant increase of the Co magnetic moment was revealed for Co layer thicknesses in the monolayer range (below about 10 monolayers which corresponds to about 2 nm Co layer thickness). However, our measurement accuracy did not allow us to observe a similar increase of the Co magnetic moment even at our smallest thickness of 1 nm.

The relative remanence (M_r/M_S) is shown in Fig. 11 as a function of the Co layer thickness for all three layered magnetic nanostructures. For each datasets, the remanence is around 0.9 for sufficiently thick Co layers whereas M_r/M_S is drastically reduced towards smaller Co layer thicknesses. The reduction of M_r/M_S can be ascribed again to the presence of SPM regions in the Co layers with the smallest thicknesses.

4.2 Coercivity

The dependence of the coercive force H_c on the thickness of one Co layer in the different layered nanostructures is shown in Fig. 12. The coercivity data fall in the range 35 to 130 Oe and the general trend is a decrease of H_c with increasing d_{Co}, at least for sufficiently large Co layer thicknesses. For the Co thin films, however, at small thicknesses the data indicate a clear reduction of the coercivity.

Early studies on the thickness dependence of the coercivity of magnetic thin films revealed [22,23] that the coercive force usually varies in an inverse manner with the magnetic layer thickness, i.e., $H_c = H_{co} + a/d^n$, where H_{co} is a coercivity contribution not depending directly on the film thickness, although sometimes a breakdown of H_c towards very thin films could also be observed. As will be detailed below, recent works on magnetic Co thin films prepared under more controlled conditions and with magnetic measurements mostly carried out in-situ (in high vacuum or in an electrolyte) by magneto-optic Kerr effect also support this picture.

Wang and coworkers [45,46] studied evaporated Co films on SiO_2 substrate and obtained $n = 0.33 \pm 0.005$ (Co thickness range 0.5 nm to 4 nm) and $n = 0.4 \pm 0.1$ (Co thickness range 2 nm to 12 nm). Camarero et al. [47] obtained $n = 1$ for Co thin films MBE-grown on a Cu(111) single crystal in the thickness range from about 1 nm to 3 nm and reported a steep H_c reduction below 1 nm Co thickness down to 0.2 nm (about 1 monolayer), with H_c becoming zero at the smallest thickness.

For electrodeposited Co thin films on Cu(100) single crystals, Schindler and Kirschner [48] reported hysteresis loops revealing an approximately linear increase of H_c from about 9 Oe (at about 0.5 nm) to 250 Oe (at about 10 nm). Pasa and coworkers [18,19,49] electrodeposited Co thin films directly on (100)-oriented Si wafers with thicknesses from 25 nm into the micrometer range and obtained $n = 1.6$ and 2.1 for small and high Co^{2+} concentration in the solution, respectively, with $H_{co} \sim 25$ Oe in both cases. When the Co film was deposited from the more concentrated solution on Si covered first with a Co(27nm) layer and then with a Cu(53nm) layer [18], a drastic reduction of the H_c values appeared in the thickness range 20 nm to 100 nm although the H_{co} value remained the same as on the Si substrate.

In a most recent study, Mangen et al. [50] found for electrodeposited Co thin films a rapid increase of H_c from zero at about 0.5 nm Co layer thickness until a maximum H_c of about 200 Oe around 4 nm thickness after which a slight H_c decrease was observed until the largest thickness (9 nm) investigated.

According to the above summarized data on the coercivity of Co thin films, it can be established that H_c indeed depends on the Co layer thickness. However, the thickness dependence and, also, the H_c value itself, can vary with deposition method, deposition parameters, substrate material and Co layer thickness range as exemplified by the data of Kim and Oliveria [51] on sputtered Fe layers. As to the thickness dependence, Min et al. [45] gave a summary of the possible models. An important starting point is that in magnetic thin films in the nanometer thickness range of interest here for us, there are domain walls only which are perpendicular to the film plane since the film thickness is well below the domain wall thickness in these magnetically fairly soft materials. This was clearly demonstrated for fcc-Co thin films grown on Cu(100) surfaces by physical deposition [52]: for 1 to 2 nm thick Co layers, the domain wall width was shown to be around 1 micrometer and the magnetization was found to be in the film plane. Therefore, the magnetization reversal process proceeds mostly with domain wall motion. For magnetic thin films, on the other hand, the type of domain walls depends on the film thickness. Since the coercivity depends on the energy of the domain wall and the wall energy depends on the domain wall type, H_c will be different for various domain wall types.

For sufficiently thick magnetic films, usually Bloch walls are present for which the standard result [22,23] for the thickness dependent part of the coercivity is $n = 4/3$ on the basis of the original concept put forward by Néel [53]. With decreasing film thickness, the wall type changes first to cross-tie walls and then to Néel type walls for very thin films [22,23,54]. In magnetic layers with thicknesses in the nanometer range of interest here, Néel walls are expected to be present. This was explicitly shown by Berger and Oepen [52] on fcc-Co/Cu(100) thin films with 1 to 2 nm thickness by using spin-polarization analysis of the secondary electrons in a scanning electron microscope (SEMPA technique).

The available standard result for the theoretical thickness dependence of H_c in Néel walls is that the coercivity is independent of thickness, i.e., $n = 0$ [23]. Although Kim and Oliveira [51] derived an expression according to which H_c linearly increases with thickness ($n = -1$), it is easy to see that their starting point based on the so-called inclusion theory elaborated for bulk ferromagnets is clearly inapplicable for the thin film case. In attempt to understand the

origin of the thickness dependence of coercivity in the nanometric magnetic films, on the other hand, we should also take into account that the coercivity depends on surface roughness as well [22,23] which may vary with preparation details and also may vary with films thickness. It is noted in this context that, recently, Gong et al. [55] have analyzed the surface roughness contribution to H_c for electrodeposited permalloy thin films.

In addition, we should also keep in mind that magnetostrictive effects due to inherent internal stresses built in during deposition, which may even vary with thickness, can also significantly contribute to the coercivity value and its thickness dependence. For example, Tabakovic et al. [56] have shown for electrodeposited Co-Ni-Fe films that the evolution of internal stress with magnetic layer thickness may be even qualitatively different (decreasing or increasing with thickness) on various substrates, which itself can provide an immediate explanation for the strong substrate dependence of their n values (ranging from 0.4 to 1.29), regardless of all other experimental conditions and layer thicknesess.

By considering all the above mentioned factors influencing thin film coercivity, practically any kind of thickness dependence of H_c can occur for magnetic thin films.

Therefore, since the majority of available thin film coercivity data exhibited an decrease of H_c with increasing film thickness, we tried to fit our Co thin films data with $d_{Co} \geq 3$ nm in Fig. 12 with the form $H_c = H_{co} + a/d^n$ and we obtained $H_{co} = 24$ Oe, $n = 0.98$ and $a = 311$ Oe·(nm)^n. The fit curve passes well through the data points and the n value is close to 1 as obtained in some cases among the above cited literature values for Co thin films. Our coercivity value at large Co thicknesses ($H_{co} = 24$ Oe) agrees well with the value of $H_{co} = 25$ Oe reported by Pasa and coworkers [18] for electrodeposited Co layers. It also corresponds well to the value (about 20 Oe) we reported [21] for electrodeposited Co/Cu multilayers with very thin, discontinuous Cu layers, i.e., practically for bulk fcc-Co. It should be noted that the data point for the Co(7nm) thin film was omitted from the fit since its inclusion resulted in an unphysical negative value for H_{co}. This very large H_c value may have occurred due to a random sample preparation problem which we have mostly attributed [57] to an occasional degradation (perhaps e.g., larger roughness) of the evaporated substrates the quality of which cannot be tested individually.

We have left out of consideration in the fitting procedure also the data for the two smallest layer thicknesses. These latter smaller H_c values may occur due to the presence of SPM regions in the Co thin film at very small layer thicknesses as was already hinted at above from conclusions based on several other measured parameters.

It can be seen that our H_c data for electrodeposited Co/Cu/Co sandwiches for $d_{Co} \geq 3$ nm (Fig. 12) follow a similar behavior than obtained for the Co thin films. The Co/Cu/Co sandwich fit parameters are as follows: H_{co} = 28 Oe, n = 1.14 and a = 297 Oe·(nm)^n. The fit parameters are fairly close to those obtained on the Co thin films. In the literature, we have not found any related coercivity data to compare with our results. For the Co/Cu/Co sandwiches, all the data for $d_{Co} \geq 3$ nm follow the trend described by $H_c = H_{co} + a/d^n$. The inclusion of data in the fit for Co layer thicknesses below 3 nm resulted again in a negative H_{co} value. This is a clear indication for a reduction of H_c towards small Co layer thicknesses which may again be ascribed to the presence of SPM regions in the magnetic layers. However, it is clear that the H_c data for the Co/Cu/Co sandwiches are somewhat smaller than those of the Co thin films.

The coercivity data of our Co/Cu multilayers also follow the same trend as the other two sample sets with H_{co} = 29 Oe, n = 0.85 and a = 110 Oe·(nm)^n. Here, the H_c value for the smallest Co layer thickness investigated (1 nm) had to be omitted from the fit to get positive H_{co}; the slightly reduced H_c value for d_{Co} = 1 nm implies some SPM contribution, again in line with previous conclusions above from other data. In general, the multilayer H_c values are the smallest among the three datasets.

In our previous work [58], a monotonous decrease of H_c was observed for electrodeposited Co/Cu multilayers in the Co layer thickness range from 1 nm to 6 nm although a quantitative comparison is not easy since the Cu layers were much thinner and the total multilayer thicknesses were much larger and the substrate was also different (polycrystalline Ti sheet).

Chowdhury et al. [36] studied the coercive field of electrodeposited Co/Cu multilayers on Si/Ta/Cu substrates with d_{Co} varying from 0.2 to 10 nm whereby the Cu layer thickness was held constant at 4 nm. They found that H_c increased with decreasing d_{Co} down to about 3 nm after which a sharp decrease of H_c followed for smaller Co layer thicknesses with H_c going practically to zero at the smallest layer thicknesses. Their coercive field values were comparable to our ones presented in Fig. 12. These authors have also ascribed the reduced H_c values to the SPM character of the magnetic layers for small d_{Co} values. Further works on electrodeposited [37] and sputtered [38-40] Co/Cu multilayers also support this picture. It is noted that a drastic drop of H_c to practically zero from about 300 Oe was observed [59] also

in electrodeposited Co-Ni/Cu multilayered nanowires when the magnetic layer thickness was reduced from 5 nm to 2 nm.

We could see above that the values of the exponent n characterizing the thickness dependence of the coercivity are scattered around 1 for all three layered magnetic nanostructures: $n = 0.98$ for Co thin films, $n = 1.14$ for Co/Cu/Co sandwiches and $n = 0.85$ for Co/Cu multilayers. Due to the experimental uncertainties which may have caused some scatter of the H_c data, a fairly common n value can be considered for all three types of layered nanostructure investigated. Since for each type of nanostructure the magnetic layer was inserted between the same Cu layers, i.e., causing the same internal stresses, the observed thickness dependence of H_c may be assumed to properly reflect the true dependence of the coercivity on magnetic layer thickness. The influence of an eventual variation of the roughness with total layered structure thickness can also be ruled out since, in an overall comparison, the 100 nm thick Co/Cu multilayers exhibited smaller coercive field values than the much thinner Co thin films and Co/Cu/Co multilayers with similar individual Co layer thicknesses. This conclusion can be made because, whereas the surface roughness of the Si/Cr/Cu substrates was fairly low (the surface did not show fluctuation larger than 3 nm), the surface roughness of very similar electrodeposited Co/Cu multilayers increased significantly with increasing total multilayer thickness [24].

The observed n value close to for each type of layered nanostructure studied here definitely deviates from the $n = 4/3$ value derived for Bloch walls and agreement is not even expected due to the fact that in the Co layer thickness range investigated, the walls are not of the Bloch type but of the Néel type [52]. At the moment, there is no theoretical model which would predict an exponent value $n = 1$ although a very large number of reports give n values close to 1. Nevertheless, the fairly common n value for the three kinds of layered magnetic nanostructures investigated here suggests for us that the magnetization reversal mechanism should be the same (or at least very similar).

Furthermore, we can also conclude from the common n value that there is no significant coupling between the Co layers in the Co/Cu/Co sandwiches and in the Co/Cu multilayers since the magnetization reversal mechanism seems to be the same. As concluded above from a discussion of the comparison of the coercivity magnitude (quantitatively represented by the fitted values of the coefficient a in the fitting expression $H_c = H_{co} + a/d^n$), there is an indication that surface roughness effects do not give a substantial contribution to the coercivity of the current layered nanostructures.

We should make, however, a remark about the roughness effect on coercivity at this point. Namely, independently of the success or failure of theoretical models in describing the thickness dependence of coercivity in magnetic thin films, the reasonable starting point as put forward by Néel [53] should consider the surface roughness on a lateral scale only which corresponds approximately to the domain wall thickness. This is because this roughness can only be effective in trapping the domain wall into a low-energy site. The length-scale of this roughness (i.e., the domain wall width) is generally a few tens of nanometer at most for magnetic thin films. However, the height fluctuations on this scale are certainly much smaller than the height fluctuations evaluated by AFM over much larger length scales [60]. Therefore, the typical AFM roughness values may not have a serious influence on the coercivity. If this is the case indeed, then it could also explain why the much thicker Co/Cu multilayers having certainly larger surface roughness on the long scale than the Co thin films and Co/Cu/Co sandwiches have even lower coercive fields compared to the values obtained for the two other layered structures.

Although the MR data will be presented in detial in the next section only, the peak field value (H_p) of the *MR(H)* curves are discussed here since H_p is usually considered to roughly correspond to the coercive field as we have already experienced for electrodeposited Co/Cu multilayers [21,58]. Although both H_c and H_p indicate some critical points of the remagnetization process, since the conditions corresponding to the critical magnetic field are defined differently for the magnetization and the magnetoresistance, their values should not necessarily be identical but at least their variation with, e.g., the Co layer thickness can be expected to show some similarity.

The H_p values for all the samples, averaged for the LMR and the TMR contributions, are plotted in Fig. 13a. The general behavior with d_{Co} is mostly very similar for that shown in Fig. 12 for H_c. The only exception is that for the Co thin films the H_p values start to decrease with decreasing d_{Co} already below about 5 nm Co layer thickness which may be again due to the larger and larger SPM contribution towards very thin Co layers. This breakdown of H_p (and also of H_c, cf. Fig. 12) for the Co thin films only and its lack for the Co/Cu/Co sandwiches and Co/Cu multilayers with comparably small Co layer thicknesses seems to underpin again that the nucleation of the very first Co layer is really crucial since this may strongly promote the appearance of SPM regions. Furthermore, the differences in the thickness ranges where the reduction of the H_c and H_p values sets in also reveal that the two parameters are sensitive to different details of the magnetization reversal process.

In order to see to what extent the H_p values correlate with H_c, the H_p data are plotted in Fig. 13b as a function of the coercivities of the same sample. The $y = x$ line is given as reference only. There is a clear correlation between the two sets of data, but evidently the scatter is also fairly large. This may be partly due to the experimental errors of both quantities and due to the differences in sensitivity of the magnetic and magnetoresistance measurements to the details of magnetization reversal mechanism as was discussed above on the basis of the explanation by Spizzo et al. [38].

4.2 Magnetoresistance

The AMR values are shown in Fig. 14 as a function of the thickness of one Co layer for all three layered structures. In general, the AMR value increases for each type of structure with increasing Co layer thickness. This is expected since for thicker magnetic layers a larger fraction of the electron scattering events stems from scatterings within the magnetic layers. The much smaller rate of increase for the Co thin films with respect to the other two structures may be due to a larger shunting effect of the conducting substrate in the case of a single Co layer.

From the *MR(H)* curves, we have extracted the saturation values of the isotropic giant magnetoresistance contribution (GMR_{is}) of the Co/Cu/Co sandwiches and the Co/Cu multilayers. The GMR_{is} data are plotted in Fig. 15 for these two layered structures. For the Co/Cu/Co sandwiches, the LMR and TMR data indicated the presence of a clear GMR contribution which was of the GMR_{FM} type. The small GMR_{is} values are mainly due to the shunting effect of the substrate. For the Co/Cu multilayers, the GMR is much higher, especially at low Co layer thicknesses since there are several Co/Cu/Co units in each sample which are the main source of electron scattering events yielding a GMR effect. The strong reduction of the GMR with increasing Co layer thickness is due to effect of reducing the number of Co/Cu/Co units since the total multilayer thickness was fixed at around 100 nm.

5. Summary

In the present work, we investigated the magnetic and magnetoresistive properties of nanometric Co thin films and Co/Cu layered structures. Electrodeposition was used to prepare Co thin films, Co/Cu/Co sandwiches and Co/Cu multilayers with individual Co layer thicknesses ranging from 1 nm to 20 nm. The layered structures were electrodeposited on Si/Cr/Cu substrates with smooth evaporated metallic layers. The last magnetic layer was always covered with a 5-nm-thick Cu layer from the electrolyte to prevent oxidation.

The Co/Cu/Co sandwiches and Co/Cu multilayers with not too thick magnetic layers exhibited dominantly a GMR behavior. The magnetoresistance data showed that in these layered structures the GMR effect decreases as the Co layer thickness increases. This is due to the decreasing number of Co/Cu interfaces per unit thickness since these interfaces are responsible for the GMR effect.

All three types of layered structure exhibited dominantly an AMR behavior for sufficiently thick magnetic layers whereby the critical Co layer thickness separating the GMR and AMR regime was different for the two structure types.

The decreasing values of the relative remanence and the coercive field when reducing the Co layer thickness down to below about 3 nm indicated the presence of SPM regions in the magnetic layers. The formation of SPM regions could be more firmly evidenced for these samples by a decomposition of the magnetoresistance vs. field curves into a ferromagnetic and an SPM contribution. The measured saturation magnetization supported reasonably the validity of the nominal layer thicknesses.

For magnetic layers with thicknesses above about 3 nm, the dependence of the coercivity on magnetic layer thickness could be described for each of the layered structure types by the usual equation $H_c = H_{co} + a/d^n$. The value of the exponent was found to be $n = 0.98$ for Co thin films, $n = 1.14$ for Co/Cu/Co sandwiches and $n = 0.85$ for Co/Cu multilayers. By considering the uncertainty of the determination of the exponent due to the scatter of the H_c values, it can be established that the n value is about 1 for each of the three layered structures.

The common value of n suggests a similar mechanism for the magnetization reversal by domain wall motion in all three structure types and hints, at the same time, for the absence of coupling between magnetic layers in the Co/Cu/Co sandwiches and Co/Cu multilayers.

Acknowledgements This work was supported by the Hungarian Scientific Research Fund (OTKA) through Grant K 104696.

References

1. M.N. Baibich, J.M. Broto, A. Fert, F. Nguyen Van Dau, F. Petroff, P. Etienne, G. Creuzet, A. Friederich and J. Chazelas, *Phys. Rev. Lett.* **61**, 2472 (1988)
2. G. Binasch, P. Grünberg, F. Saurenbach and W. Zinn, *Phys. Rev. B* **39**, 4828 (1989)
3. B. Dieny, V.S. Speriousu, S.S.P. Parkin, B.A. Gurney, D.R. Wilhoit and D. Mauri, *Phys. Rev. B* **43**, 1297 (1991); B. Dieny, *J. Magn. Magn. Mater.* **136**, 335 (1994)
4. I. Bakonyi and L. Péter, *Progr. Mater. Sci.* **55**, 107 (2010)
5. J.M. Daughton and Y.J. Chen, IEEE Trans. Magn. **29**, 2705 (1993); J.M. Daughton, *J. Magn. Magn. Mater.* **192**, 334 (1999)
6. J. Barnas, O. Baksalary, and A. Fert, *Phys. Rev. B* **56**, 6079 (1997)
7. C. Blaas, P. Weinberger, L. Szunyogh, J. Kudrnovsky, V. Drchal, P. M. Levy, and C. Sommers, Eur. Phys. J. B **9**, 245 (1999)
8. K. Szász and I. Bakonyi, *J. Spintr. Magn. Nanomater.* **1**, 159 (2012)
9. D.H. Mosca, F. Petroff, A. Fert, P.A. Schroeder, W.P. Pratt Jr. and R. Laloee, *J. Magn.. Magn. Mater.* **94**, L1 (1991)
10. S.S.P.Parkin, R. Bhadra and K.P. Roche, *Phys. Rev. Lett.* **66**, 2152 (1991)
11. H. Kubota, S. Ishio, T. Miyazaki and Z.M. Stadnik, *J. Magn. Magn. Mater.* **129**, 383 (1994)
12. T. Shinjo and H. Yamamoto, *J. Phys. Soc. Jpn.* **59**, 3061 (1990)
13. B. Dieny, V.S. Speriosu, B.A. Gurney, S.S.P. Parkin, D.R. Wilhoit, K.P. Roche, S. Metin, D.T. Peterson and S. Nadimi, *J. Magn. Magn. Mater.* **93**, 101 (1991)
14. K. Attenborough, H. Boeve, J. de Boeck, G. Borghs and J.-P. Celis, *Appl. Phys. Lett.* **74**, 2206 (1999)
15. K. Attenborough, H. Boeve, J. De Boeck, G. Borghs and J.P. Celis, *IEEE Trans. Magn.* **35**, 3094 (1999)
16. K. Attenborough, H. Boeve, J. de Boeck, G. Borghs and J.-P. Celis, *Sensors and Actuators* **81**, 9 (2000)
17. M. Shima, L.G. Salamanca-Riba, T.P. Moffat and R.D. McMichael, In: *Magnetic Materials, Processes, and Devices V*. Eds. L.T. Romankiw, S. Krongelb, and C. H. Ahn (The Electrochemical Society Proceedings Series, Pennington, NJ, USA, 1999), PV 98-20, p. 176.
18. A.A. Pasa, M.L. Munford, E Voltolini, L. Seligman, M. Sardela and M.L. Sartorelli, in: *Magnetic Materials, Processes, and Devices VI*. Eds. S. Krongelb, L.T. Romankiw, J.-W. Chang, W. Schwarzacher and C.H. Ahn (The Electrochemical Society Proceedings Series, Pennington, NJ, USA, 2001), PV 2000-29, p. 137.
19. L. Seligman, M.L. Sartorelli, A.A. Pasa, W. Schwarzacher and O.I. Kasyutich, *J. Magn. Magn. Mater.* **226**, 752 (2001)
20. S.K.J. Lenczowski, C. Schönenberger, M.A.M. Gijs and W.J.M. de Jonge, *J. Magn. Magn. Mater.* **148**, 455 (1995)
21. I. Bakonyi, E. Simon, B.G. Tóth, L. Péter and L.F. Kiss, *Phys. Rev. B* **79**, 174421 (2009)
22. M. Prutton, *Thin Ferromagnetic Films* (Butterworths, London, 1964)
23. R.F. Soohoo, *Magnetic Thin Films* (Harper & Row, New York, 1965)
24. B.G. Tóth, L. Péter, I. Bakonyi, *J. Electrochem. Soc.* **158**, D671 (2011)
25. V. Weihnacht**,** L. Péter, J. Tóth, J. Pádár, Zs. Kerner, C.M. Schneider and I. Bakonyi, *J. Electrochem. Soc.* **150**, C507 (2003)
26. B.G. Tóth, L. Péter, Á. Révész, J. Pádár, I. Bakonyi, *Eur. Phys. J. B* **75**, 167 (2010)
27. D. Rafaja, C. Schimpf, V. Klemm, G. Schreiber, I. Bakonyi, L. Péter, *Acta Mater.* **57**, 3211 (2009)
28. D. Rafaja, C. Schimpf, T. Schucknecht, V. Klemm, L. Péter, I. Bakonyi, *Acta Mater.* **59**, 2992 (2011)
29. R.M. Bozorth, *Ferromagnetism* (Van Nostrand, New York, 1951)
30. T.R. McGuire and R.I. Potter, *IEEE Trans. Magn.* **11**, 1018 (1975)
31. B. Raquet, M. Viret, J.M. Broto, E. Sondergard, O. Cespedes and R. Mamy, *J. Appl. Phys.* **91**, 8129 (2002); B. Raquet, M. Viret, E. Sondergard, O. Cespedes and R. Mamy, *Phys. Rev. B* **66**, 024433 (2002)
32. I. Bakonyi, L. Péter, Z. Rolik, K. Kiss-Szabó, Z. Kupay, J. Tóth, L.F. Kiss and J. Pádár, *Phys. Rev. B* **70**, 054427 (2004)

33. L. Péter, Z. Rolik, L.F. Kiss, J. Tóth, V. Weihnacht, C.M. Schneider and I. Bakonyi, *Phys. Rev. B*; **73**, 174401 (2006)
34. Q.X. Liu, L. Péter, J. Pádár, I. Bakonyi, *J. Electrochem. Soc.* **152**, C316 (2005)
35. L. Péter, V. Weihnacht, J. Tóth, J. Pádár, L. Pogány, C.M. Schneider and I. Bakonyi, *J. Magn. Magn. Mater.* **312**, 258 (2007)
36. P. Chowdhury, S.K. Ghosh, A. Dogra, G.K. Dey, Y.G. Gowda, S.K. Gupta, G. Ravikumar, A.K. Grover and A.K. Suri, *Phys. Rev. B* **77**, 134441 (2008)
37. S.K. Ghosh, P. Chowdhury and A. Dogra, *J. Magn.. Magn. Mater.* **327**, 121 (2013)
38. F. Spizzo, E. Angeli, D. Bisero, P. Vavassori and F. Ronconi, *Appl. Phys. Lett.* **79**, 3293 (2001)
39. F. Spizzo, E. Angeli, D. Bisero, P. Vavassori and F. Ronconi, *J. Magn. Magn. Mater.* **242-245**, 473 (2002)
40. P. Vavassori, F. Spizzo, E. Angeli, D. Bisero and F. Ronconi, *J. Magn. Magn. Mater.* **262**, 120 (2003)
41. X. Liu, M.M. Steiner, R. Sooryakumar, G.A. Prinz, R.F.C. Farrow and G. Harp, *Phys. Rev. B* **53**, 12166 (1996)
42. P. Bödecker, A. Abromeit, K. Bröhl, P. Sonntag, N. Metoki and H. Zabel, *Phys. Rev. B*; **47**, 2353 (1993)
43. S. Topolovec, H. Krenn and R. Würschum, *J. Magn. Magn. Mater.* **397**, 96 (2016)
44. M.B. Stearns, in: H.P.J.Wijn (Ed.), Landolt-Börnstein — Group III Condensed Matter, (Springer, Heidelberg, 1986) **19a**, p. 37, http://dx.doi.org/10.1007/10311893_7.
45. H.G. Min, S.H. Kim, M. Li, J.B. Wedding and G.C. Wang, *Surc. Sci.* **400**, 19 (1998)
46. M. Li and G.C. Wang, *J. Magn.. Magn. Mater.* **217**, 199 (2000)
47. J. Camarero, J.J. de Miguel, R. Miranda and A. Hernando, *J. Phys.: Cond. Matter.* **12**, 7713 (2000)
48. W. Schindler and J. Kirschner, *Phys. Rev. B.* **55**, R1989 (1997)
49. M.L. Munford, M.L. Sartorelli, L. Seligman, A.A. Pasa, *J. Electrochem. Soc.* **149**, C274 (2002)
50. T. Mangen, H.S. Bai and J.S. Tsay, *J. Magn.. Magn. Mater.* **322**, 1863 (2010)
51. Y.K. Kim and M. Oliveira, *J. Appl. Phys.* **74**, 1233 (1993)
52. A. Berger and H.P. Oepen, Phys. Rev. B**45**, 12596 (1992)
53. L. Néel, J. Phys. Radium17, 250 (1956)
54. A. Hubert and R. Schäfer, *Magnetic Domains* (Springer-Verlag, Berlin, 1998)
55. J. Gong, S. Riemer, M. Kautzky and I. Tabakovic, *J. Magn. Magn. Mater.* **398**, 64 (2016)
56. I. Tabakovic, V. Inturi and S. Riemer, *J. Electrochem. Soc.* **149**, C18 (2002)
57. K. Neuróhr, L. Péter, L. Pogány, D. Rafaja, A Csik, K. Vad, G. Molnár and I. Bakonyi, *J. Electrochem. Soc.* **162**, D331 (2015)
58. Q.X. Liu, L. Péter, J. Tóth, L.F. Kiss, Á . Cziráki, and I. Bakonyi, *J. Magn. Magn. Mater.* **280**, 60 (2004)
59. X.T. Tang, G.C. Wang and M. Shima, *J. Appl. Phys.* **99**, 123910 (2006)
60. W. Schwarzacher, *J. Phys.: Condens. Matter* **16**, R859 (2004)

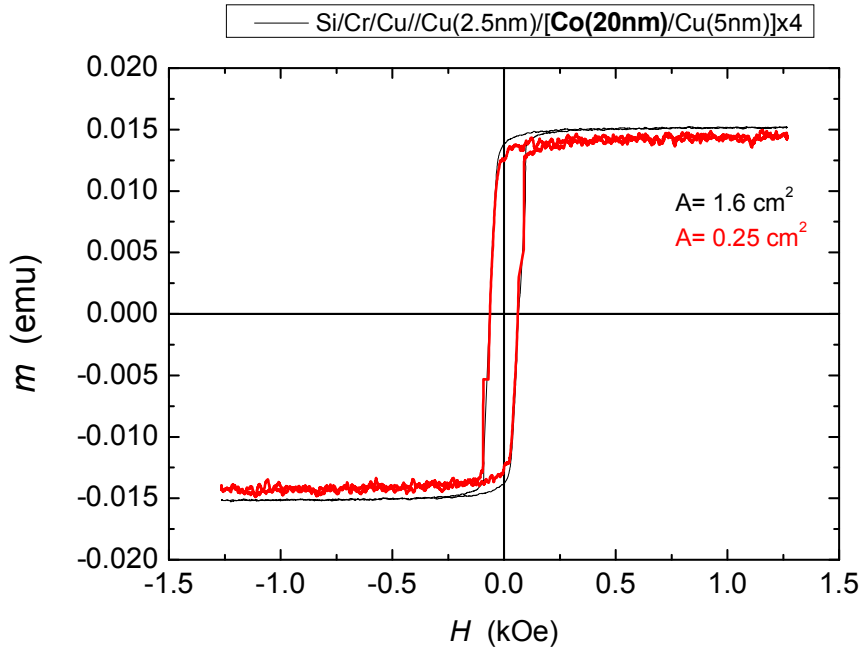

Figure 1 Magnetic hysteresis loops for a [Co(20nm/Cu(5nm)]×4 multilayer when measured on the whole sample of size 8 mm × 20 mm (black curve, A =1.6 cm^2) and on the 5 mm × 5 mm central part of the same sample (red curve, A =0.25 cm^2). The magnetization data for the latter central part of the sample have been multiplied by the area ratio 1.6/0.25. The coercive field values were in good agreement (64 Oe for the full sample size and 63 Oe for the small central part). The apparent difference in the measured magnetic moments may be ascribed to an inaccuracy of the sample area estimates.

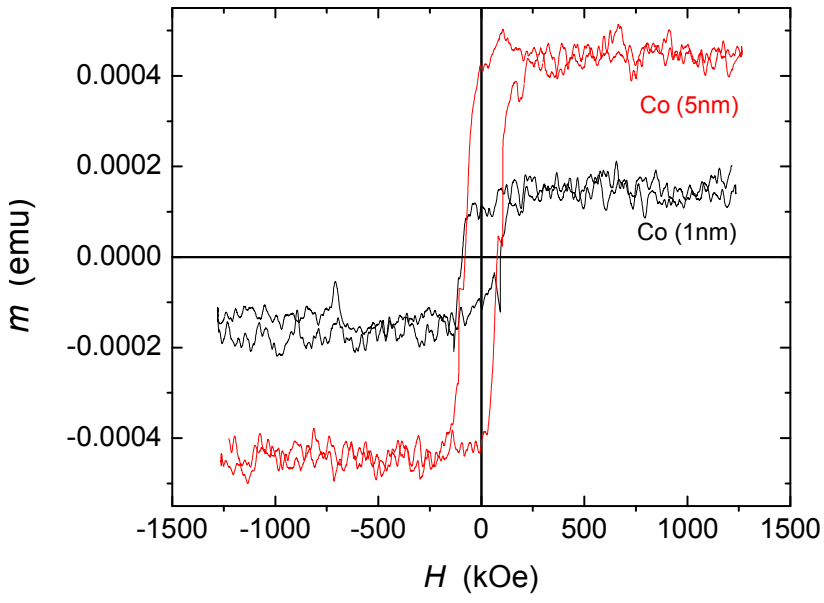

Figure 2 Magnetic hysteresis loops for Co thin films with 1 nm (black curve) and 5 nm (red curve) layer thickness.

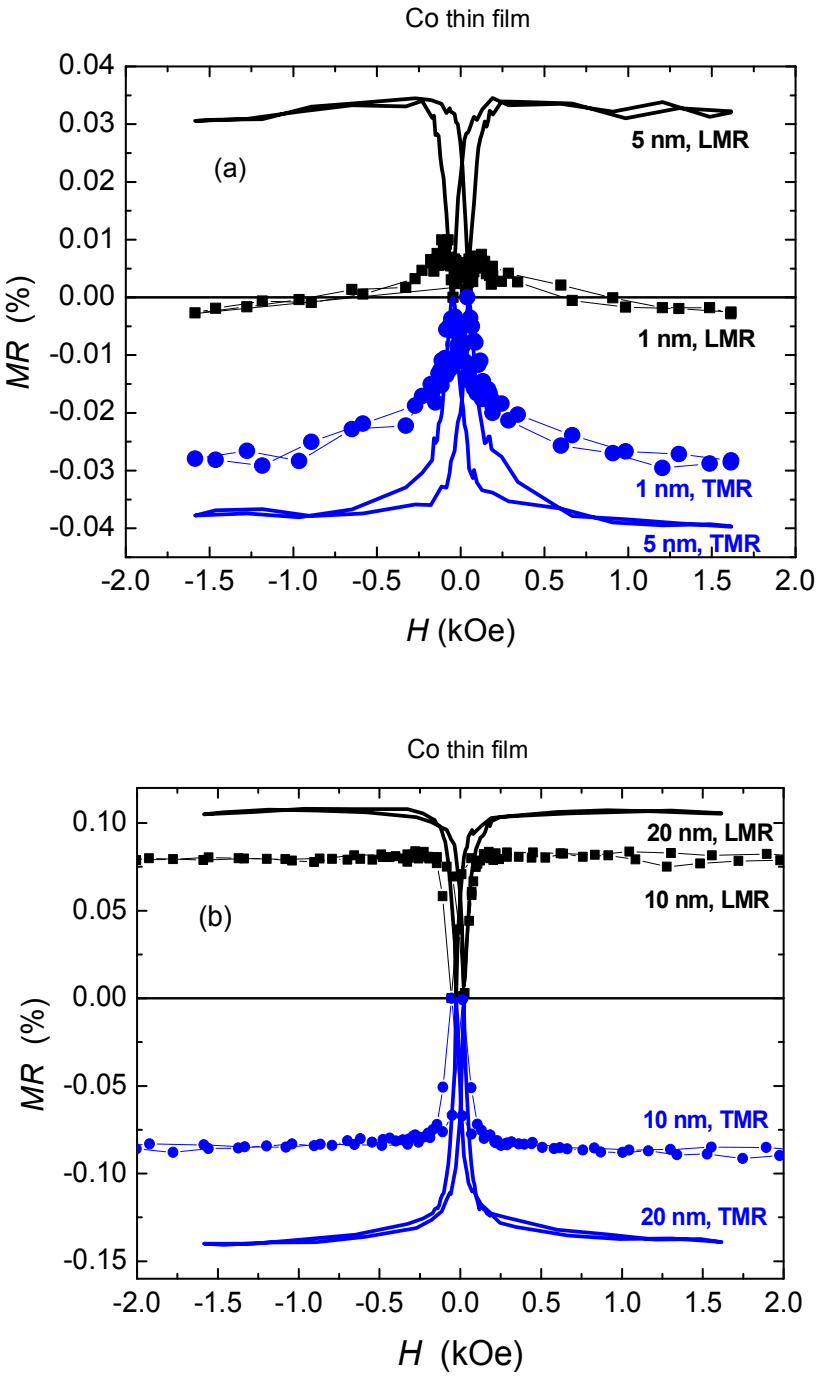

Figure 3 Magnetoresistance curves for Co thin films (a) with 1 nm and 5 nm layer thicknesses and (b) with 10 nm and 20 nm layer thicknesses.

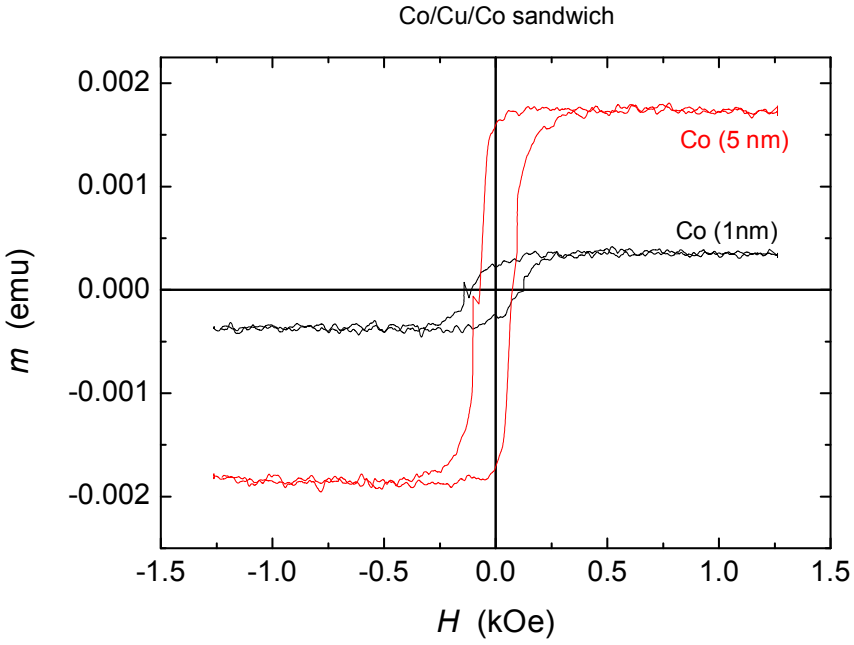

Figure 4 Magnetic hysteresis loops for Co/Cu/Co sandwiches with 1 nm (black curve) and 5 nm (red curve) thick Co layers.

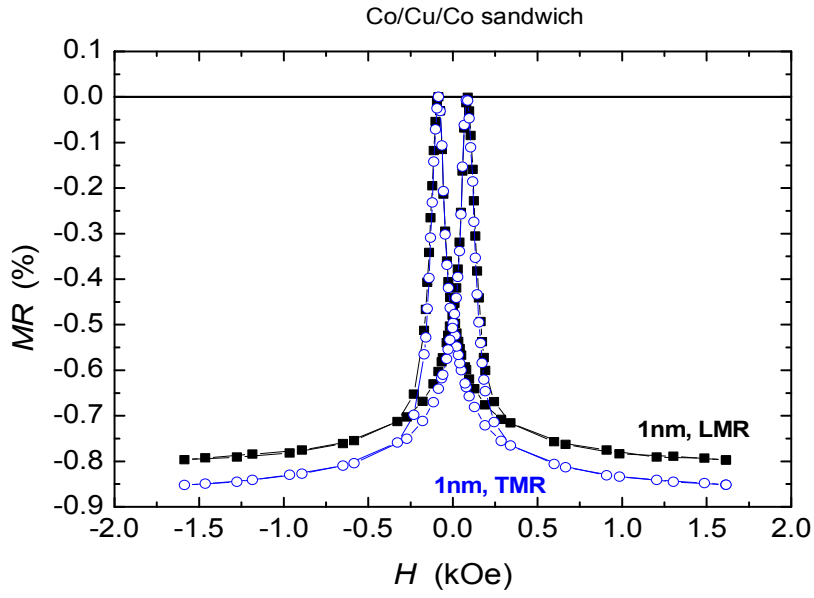

Figure 5 Magnetoresistance curves for a Co/Cu/Co sandwich with 1 nm thick Co layers.

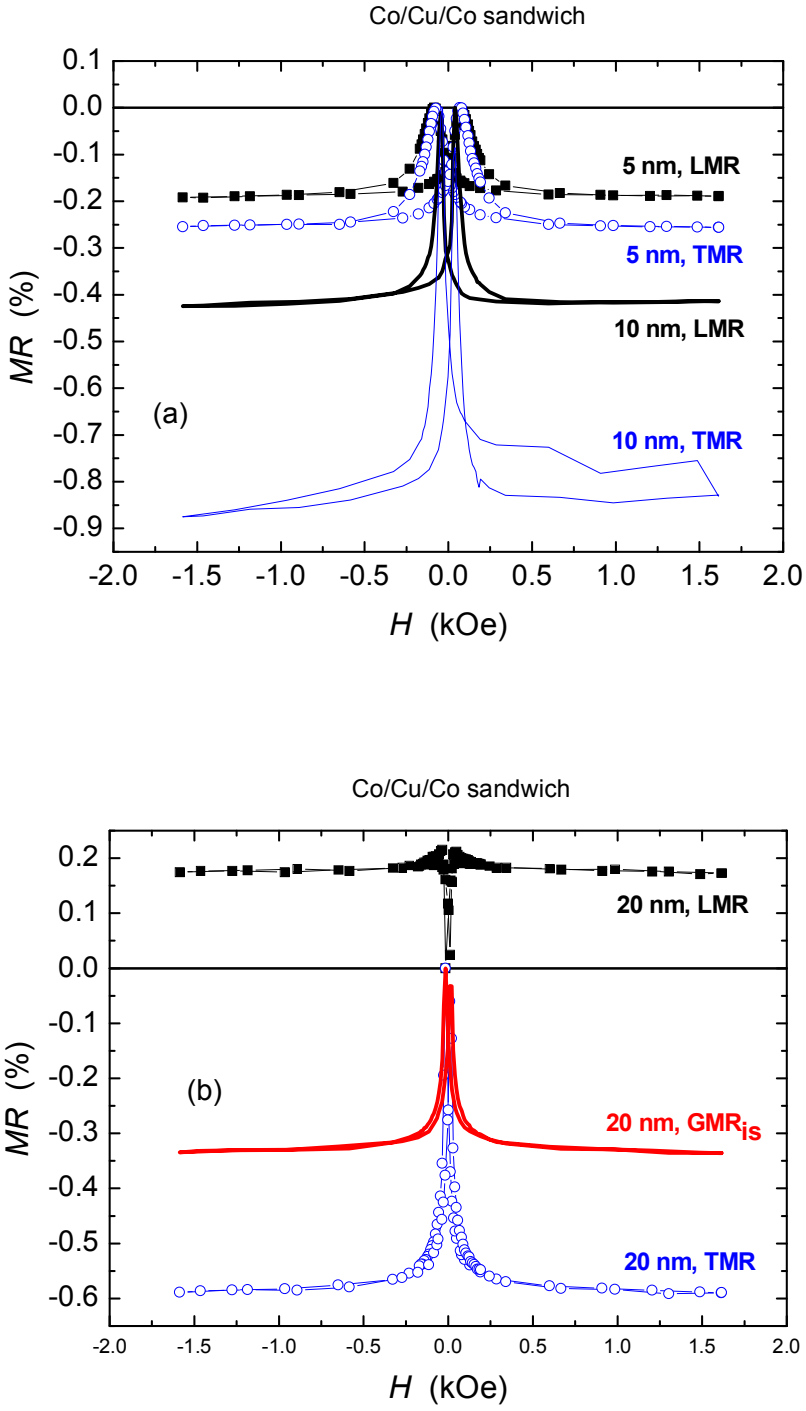

Figure 6 Magnetoresistance curves for Co/Cu/Co sandwiches (a) with 5 nm and 10 nm thick Co layers and (b) with 20 nm thick Co layers. In (b), the red curve indicates the isotropic GMR contribution obtained from the measured data as $GMR_{is}(H) = (1/3)\ LMR(H) + (2/3)\ TMR(H)$.

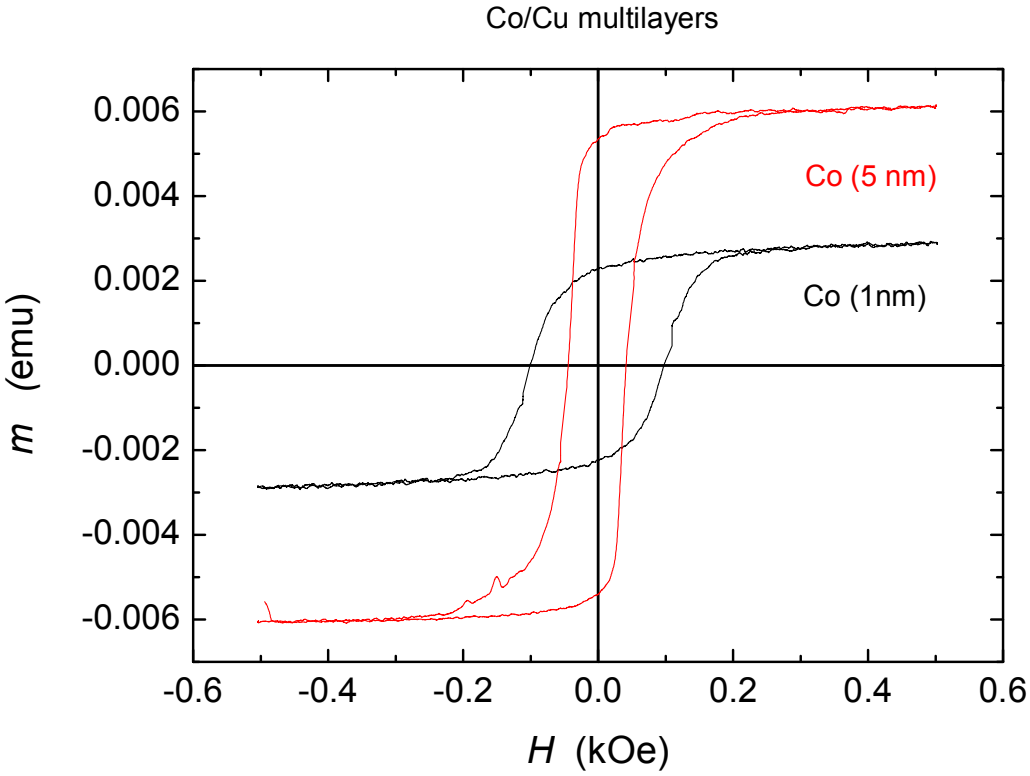

Figure 7 Magnetic hysteresis loops for Co/Cu multilayers with 1 nm (black curve) and 5 nm (red curve) thick Co layers.

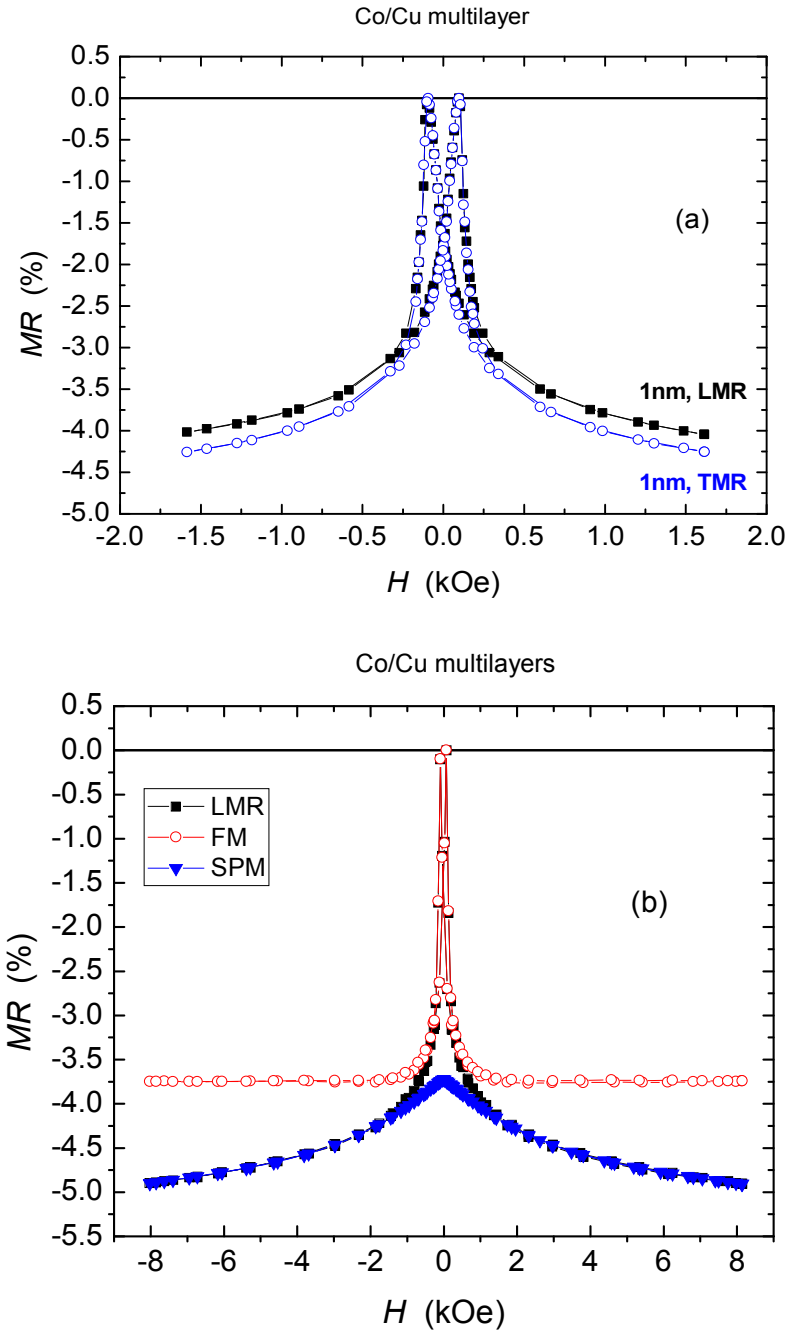

Figure 8 (a) Longitudinal and transverse magnetoresistance curves for a Co/Cu multilayer with 1 nm thick Co layers; (b) Decomposition of the LMR component (black data) of the magnetoresistance for the same sample measured up to H = 8 kOe into FM (red data) and SPM (blue data) contributions.

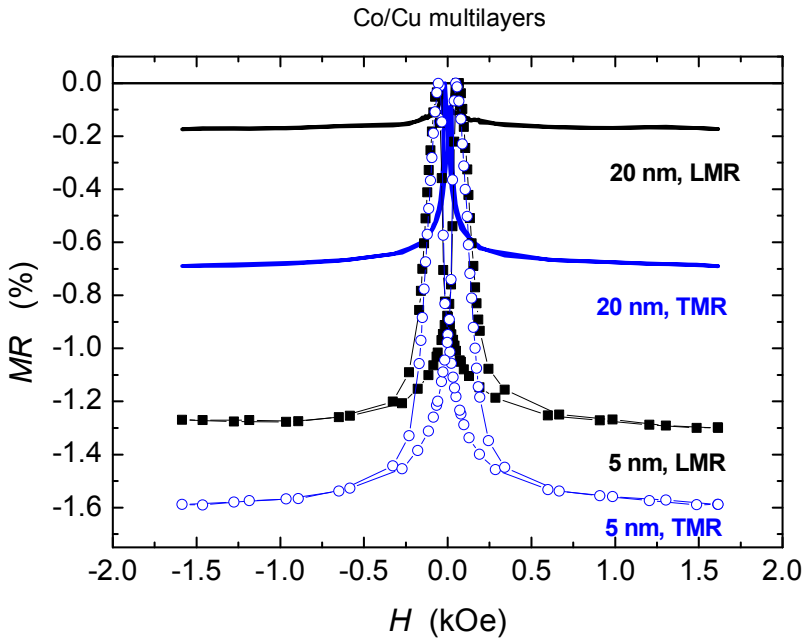

Figure 9 Magnetoresistance curves for Co/Cu multilayers with 5 nm and 20 nm thick Co layers.

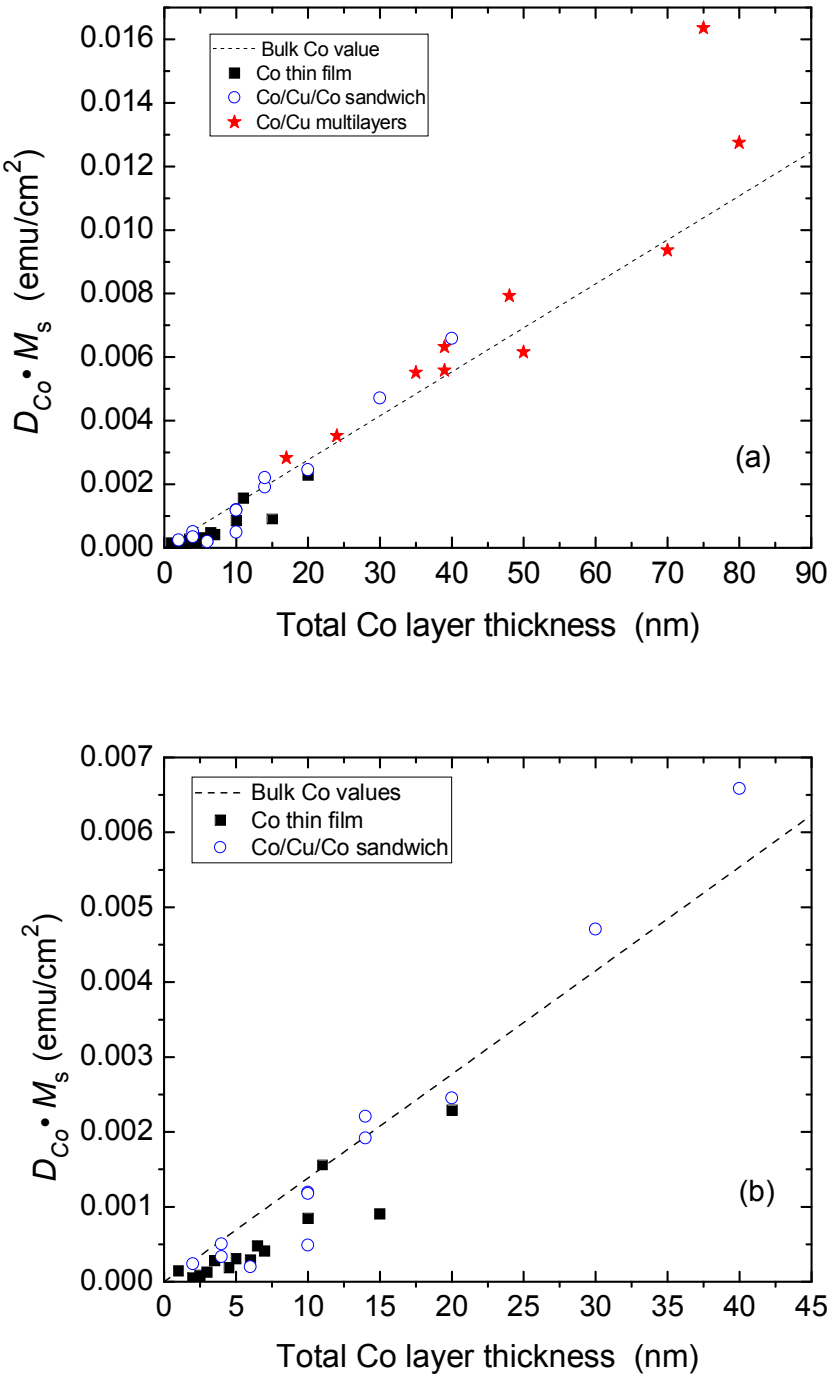

Figure 10 (a) Dependence of the measured saturation magnetization per unit area ($D_{Co} \cdot M_s$) on the total Co layer thickness for Co thin films (■), Co/Cu/Co sandwiches (○) and Co/Cu multilayers (★). The dashed reference line represents the bulk Co data; (b) The data at larger magnifications for Co thin films (■) and Co/Cu/Co sandwiches (○).

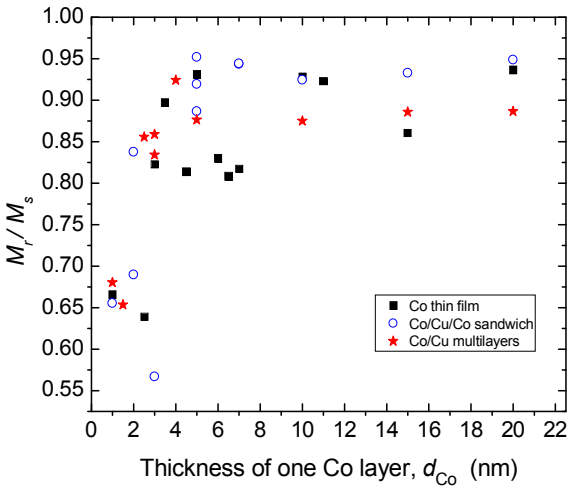

Figure 11 Dependence of the relative remanent magnetization (M_r/M_s) on the thickness of one Co layer for Co thin films (■), Co/Cu/Co sandwiches (○) and Co/Cu multilayers (★).

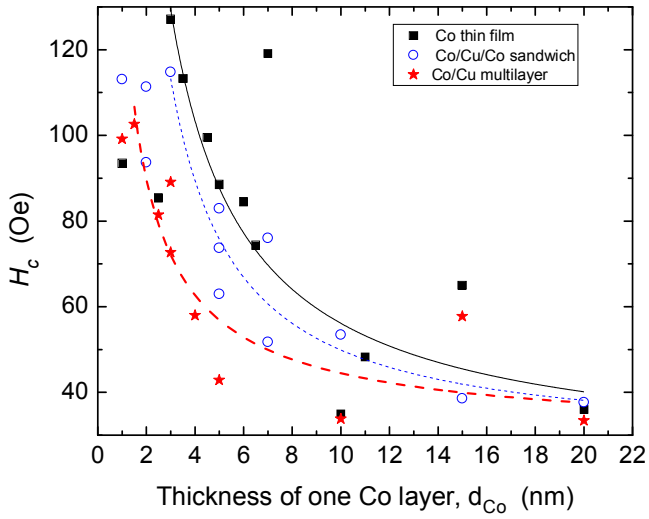

Figure 12 Dependence of the coercivity (H_c) on the thickness of one Co layer for Co thin films (■), Co/Cu/Co sandwiches (○) and Co/Cu multilayers (★). The black, blue (dotted) and red (dashed) lines represent fits to the function $H_c = H_{co} + a/d^n$ for the Co thin film, Co/Cu/Co sandwich and Co/Cu multilayer data, respectively, above a threshold Co layer thickness; for the Co thin films, the data point for d_{Co} = 7 nm was also omitted from the fit (see text).

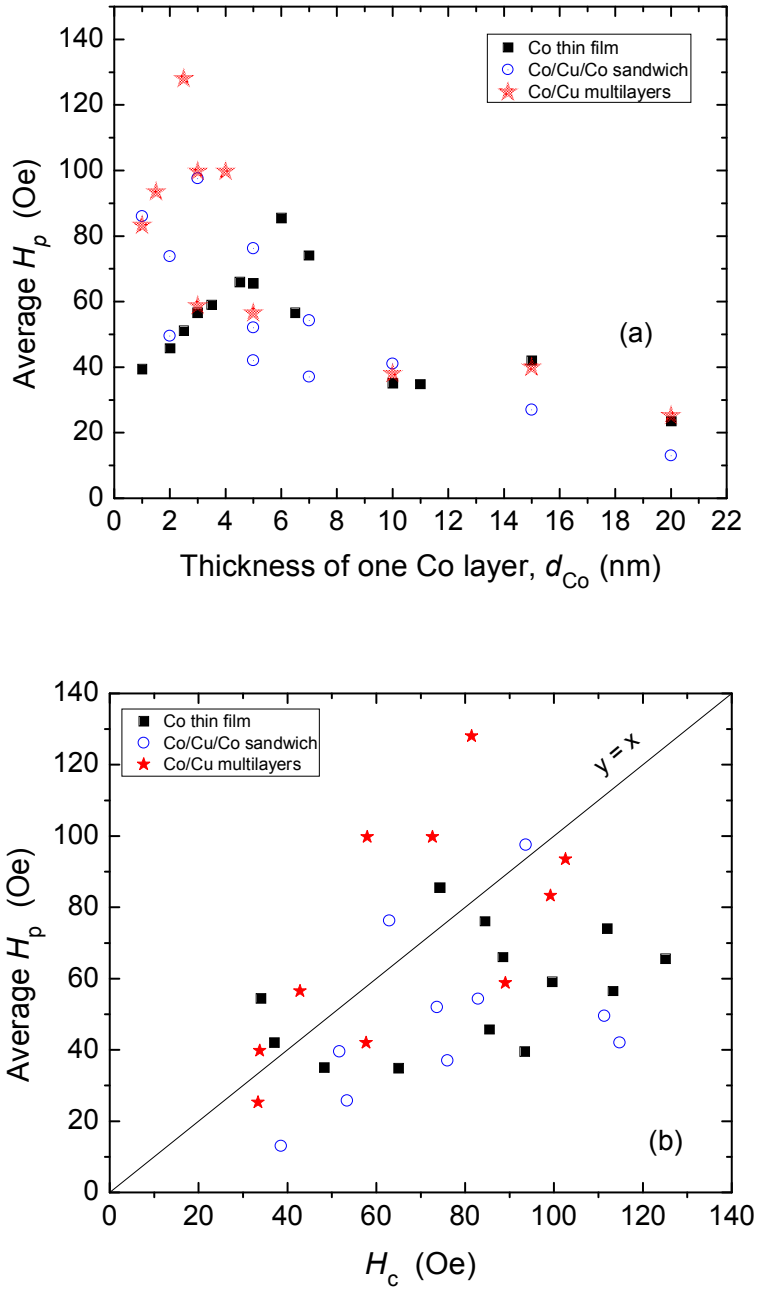

Figure 13 (a) Dependence of the peak position (H_p) of the MR(H) curves on the thickness of one Co layer for Co thin films (■), Co/Cu/Co sandwiches (○) and Co/Cu multilayers (★); (b) Correlation of the H_p and H_c values for Co thin films (■), Co/Cu/Co sandwiches (○) and Co/Cu multilayers (★).

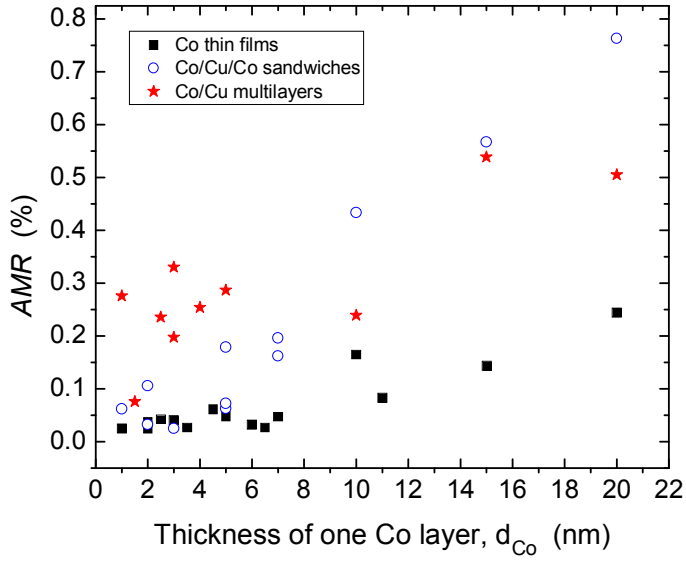

Figure 14 Dependence of the AMR on the thickness of one Co layer for Co thin films (■), Co/Cu/Co sandwiches (○) and Co/Cu multilayers (★).

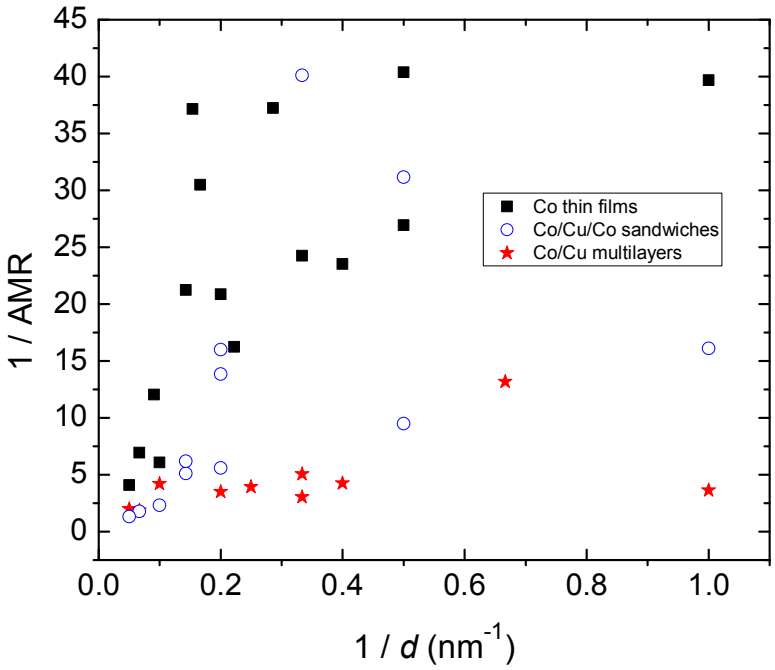

Figure 14x Dependence of the inverse of the AMR on the inverse of the thickness of one Co layer for Co thin films (■), Co/Cu/Co sandwiches (○) and Co/Cu multilayers (★).

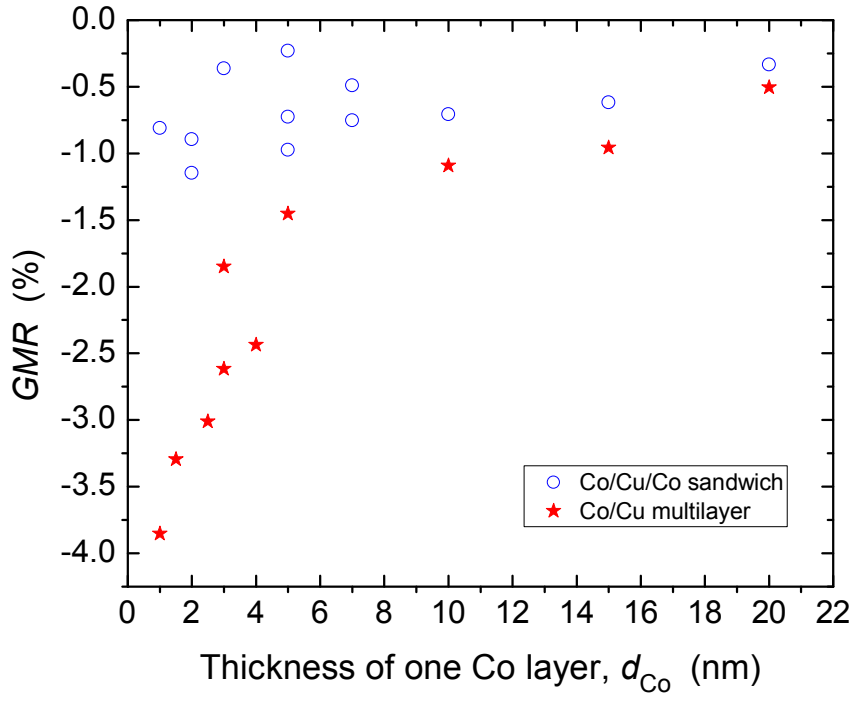

Figure 15 Dependence of the saturation value of GMR_{is} on the thickness of one Co layer for Co/Cu/Co sandwiches (○) and Co/Cu multilayers (★).